A Theoretical Study on the Substrate Deacylation Mechanism of Class C β-Lactamase

Masayuki Hata,* Yoshikazu Tanaka, Yasuyuki Fujii,† Saburo Neya, and Tyuji Hoshino

Department of Physical Chemistry, Graduate School of Pharmaceutical Sciences, Chiba University, Chiba 263-8522, Japan

Received: October 8, 2004; In Final Form: June 19, 2005

The whole reaction of the deacylation of class C β-lactamase was investigated by performing quantum chemical calculations under physiological conditions. In this study, the X-ray crystallographic structure of the inhibitor moxalactam-bound class C β-lactamase (Patera et al. *J. Am. Chem. Soc.* **2000**, *122*, 10504−10512.) was utilized and moxalactam was changed into the substrate cefaclor. A model for quantum chemical calculations was constructed using an energy-minimized structure of the substrate-bound enzyme obtained by molecular mechanics calculation, in which the enzyme was soaked in thousands of TIP3P water molecules. It was found that the deacylation reaction consisted of two elementary processes. The first process was formation of a tetrahedral intermediate, which was initiated by the activation of catalytic water by Tyr150, and the second process was detachment of the hydroxylated substrate from the enzyme, which associated with proton transfer from the side chain of Lys67 to Ser64O_γ. The first process is a rate-determining process, and the activation energy was estimated to be 30.47 kcal/mol from density functional theory calculations considering electron correlation (B3LYP/6-31G**). The side chain of Tyr150 was initially in a deprotonated state and was stably present in the active site of the acyl−enzyme complex, being held by Lys67 and Lys315 cooperatively.

1. Introduction

β-Lactamases are produced by pathogenic bacteria and are enzymes that cause resistance to β-lactam antibiotics by hydrolyzing their β-lactam rings to inactive them.[1] β-lactamases are classified into two major types on the basis of the main component of the active site: serine-β-lactamase and metallo-β-lactamase.[2] Serine-β-lactamases are further classified into three classes: classes A, C, and D. Class C β-lactamase is one of the serine-β-lactamases and is called cephalosporinase because it mainly hydrolyzes the β-lactam ring of cephalosporin compounds.

As is well-known, the catalytic mechanism of serine-β-lactamases, including class C β-lactamase, involves acylation (Scheme 1, a to c via b) and deacylation (Scheme 1, c to d). The acylation mechanism has been examined in many experimental[3−9] and theoretical works,[8,10−17] and acylation is common to serine-β-lactamase and penicillin-binding protein (PBP). Deacylation, on the other hand, is only seen in serine-β-lactamase. This means that the essence of antibiotic resistance by serine-β-lactamase arises from the deacylation reaction. Hence, an understanding of the reaction mechanism of deacylation is important for developing novel β-lactam antibiotics and potent β-lactamase inhibitors.

In our earlier work, we examined the deacylation mechanism of class A β-lactamase in detail. Hata et al.[18] performed ab initio molecular orbital (MO) calculations to elucidate the mechanism by which the acyl−enzyme tetrahedral intermediate (TI) is formed in the catalytic deacylation process of class A β-lactamase. They found that Glu166 played a role in holding a water molecule for deacylation and that a hydrogen-bond network of Lys73N_ζ−Ser130O_γ−C_3 carboxyl group of a substrate was formed after the introduction of the substrate to the enzyme and it lowered the activation energy of the tetrahedral intermediate formation reaction. Fujii and Hata et al.[19] determined the potential energy profile and structural changes in the whole reaction of deacylation by using density functional theory (DFT) calculations with the self-consistent reaction field (SCRF) theory based on the Onsager model[20−22] to take into account the environmental effect inside a protein. It was clarified from their study that not only Glu166 but also Lys73 had an important role in the deacylation reaction. They suggested that the deacylation reaction is a substrate-assisted catalytic process because the C_3 carboxyl group of the substrate also participated in the deacylation reaction.

SCHEME 1: Substrate Inactivation Mechanism by Serine-β-lactamase

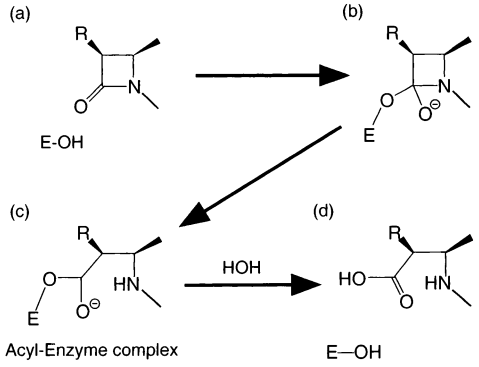

A similar deacylation mechanism is expected for class C β-lactamase, because class C β-lactamase is also a serine-β-lactamase. However, as seen in X-ray crystallographic analysis structures of class C β-lactamase,[23−28] there is no acidic amino acid residue corresponding to Glu166 in class A in the active

* Corresponding author. Phone: +81-43-290-2927. Fax: +81−43−290−2925. E-mail: hata@faculty.chiba-u.jp

† Current address: Integrated Database Team, Japan Biological Information Research Center (JBIRC), Japan Biological Information Consortium (JBIC), National Institute of Advanced Industrial Science and Technology (AIST), Time24 Bldg. 10F, Aomi 2-45, Koto-ku, Tokyo 135-0064, Japan.

10.1021/jp045403q CCC: $30.25
Published on Web 07/29/2005

SCHEME 2: R2 Group Eliminated Moxalactam (MOX) and Cefaclor (Ccl)

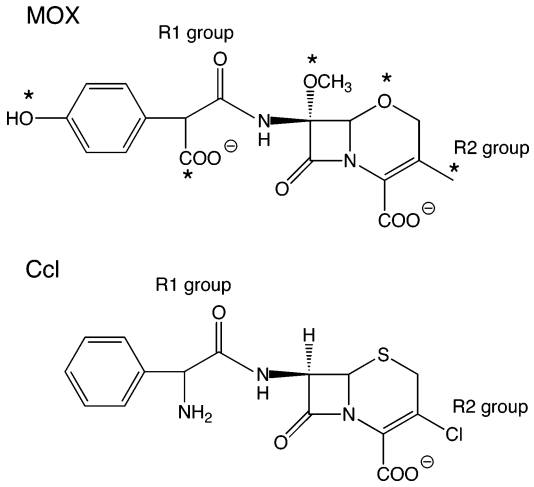

site, while a residue corresponding to Lys73 in class A is seen (Lys67). In place of Glu166 in class A, a tyrosine residue (Tyr150) exists in the active site of class C. Some authors[5,23,29] have suggested that the side chain of Tyr150 is in a deprotonated state due to the special surrounding environment of class C and plays a role as a general base. Is it true that a deprotonated state can exist stably in the active site in the process of deacylation?

In this study, we aimed to clarify the deacylation mechanism of class C β-lactamase at the atomic level through theoretical calculations. Recently, Gherman et al. obtained transition state structures for the tetrahedral intermediate formation in deacylation by class C β-lactamase and estimated the activation energies of the reaction by using quantum mechanical/molecular mechanical (QM/MM) calculations.[30] However, their calculations were only for the tetrahedral intermediate formation process, and they did not consider the whole process of deacylation. Although there have been some other QM/MM studies on enzymatic reactions,[14,31−34] there have been few studies in which the whole process of the reaction was investigated. Since it seems to be difficult to elucidate the whole process of deacylation by current QM/MM technology, we used quantum chemical calculation to elucidate the deacylation mechanism of class C β-lactamase.

2. Methods

2.1. Construction of a Model for Calculations. First, MM calculations were performed on the whole structure of the substrate-bound enzyme to construct a model for quantum chemical calculations. There is no three-dimensional crystal structure on the complex of wild-type class C β-lactamase and its substrate because reaction intermediate structures could not be detected in the experiment. However, data on the three-dimensional structure of the complex of class C β-lactamase and its inhibitor[23−28] have been reported and deposited in the Protein Data Bank.[35] In this study, an X-ray crystallographic structure of the inhibitor moxalactam-bound class C β-lactamase (PDB ID 1FCO)[24] was utilized. Because the R2 group of moxalactam is eliminated in the X-ray structure, the inhibitor (MOX) has structural similarity with cefaclor (Ccl), a substrate (Scheme 2).[36] Using this crystallographic structure, a model for MM calculations was constructed by replacing the atoms shown by asterisks in Scheme 2 to change MOX into Ccl and by generating TIP3P water molecules[37] around the enzyme using the "solvateShell" command of the LEAP module of the

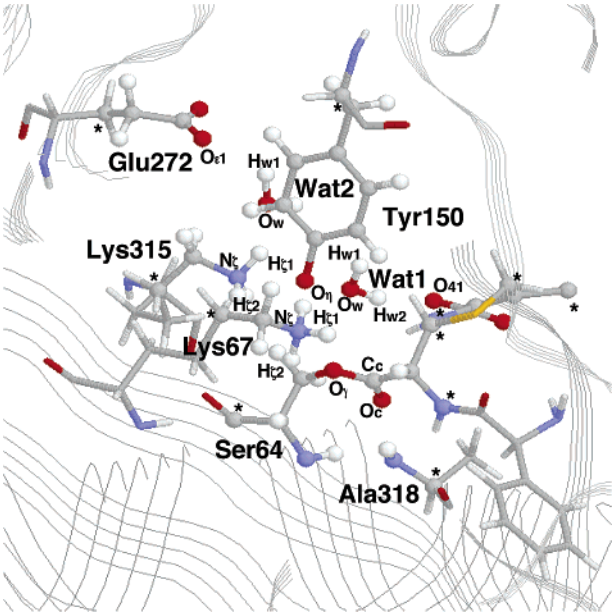

Figure 1. Active site of the acyl−enzyme intermediate structure obtained by MM calculations. Atoms shown by balls were used for the initial model for quantum chemical calculations. Atoms shown by asterisks were substituted by hydrogen atoms in the construction of a model compound.

AMBER6.0 computational program package.[38] The thickness of water molecules was 15 Å and the total number of water molecules was about 6300. The side chain of Tyr150 was treated as being in a deprotonated state. Recently, Gherman et al. proposed a Tyr150/Lys67 general base mechanism for the tetrahedral intermediate formation in deacylation of class C β-lactamase; i.e., the side chains of Tyr150 and Lys67 are neutral in the initial state of deacylation and a proton relay from the water molecule for deacylation to Lys67 via Tyr150 occurs in the tetrahedral intermediate formation.[30] However, as discussed later, the initial structure of the Tyr150/Lys67 general base mechanism had a higher level of energy than that of the Tyr150 general base mechanism (this study) at the DFT (B3LYP/6-31G**) level, which agreed qualitatively with their results. For this reason, only the Tyr150 general base mechanism was considered in this study. MM calculations were performed by using an AMBER6.0[38] computational program package. The force field parameter utilized was parm94.dat. Point charges of the substrate-bound Ser64 and the deprotonated Tyr150 were determined by the RESP module[39] of the AMBER6.0 program package. The electrostatic potential at points selected according to the Merz−Shigh−Kollman scheme[40] for use in the RESP module was calculated at the RHF/6-31G** level of theory. The computational program used was Gaussian 98.[41] For point charges of the other residues, the residue database of AMBER6.0 was utilized. The cutoff distance for nonbonded interaction was 12 Å in order to save computer resources. The energy minimization algorithm adopted was the steepest descent method (15 000 steps) followed by the conjugate gradient method (3000 steps). The model structure was fully minimized under the conditions stated above. The active site of the energy-minimized structure and important interatomic distances are shown in Figure 1 and Table 1(MM), respectively. A water molecule (Wat1) that would be involved in the substrate deacylation of class C β-lactamase was held by a hydrogen bond with Tyr150O_η (2.90 Å) and interacted with a carbonyl carbon atom of the substrate (3.71 Å). Moreover, a hydrogen-bond network was formed from Ser64O_γ to Glu272$O_{\epsilon 1}$ via Lys67N_ζ, Tyr150O_η,

TABLE 1: Important Interatomic Distances in the Potential Energy Minima and the Transition State Structures Obtained by MM and IRC Calculations

interatomic distance (Å)	MM	S1	TS1	TI1	TI2	TS2	S2
$Wat1O_w-CclC_c$	3.71	2.47	1.77	1.48	1.46	1.40	1.32
$Wat1O_w-Tyr150O_\eta$	2.90	2.69	2.51	2.77	2.74	2.86	3.53
$Wat1O_w-CclO_{41}$	2.83	3.24	3.46	3.34	3.28	3.20	2.93
$Wat1H_{w2}-CclO_{41}$	1.88	2.38	2.57	2.51	2.48	2.41	2.19
$Wat1H_{w1}-Tyr150O_\eta$	2.56	1.75	1.03	0.97	0.97	0.96	0.96
$Ser64O_\gamma-Lys67H_{\zeta2}$	2.13	2.09	2.05	2.05	1.68	1.45	0.96
$Ser64O_\gamma-Lys67N_\zeta$	2.69	2.88	2.81	2.78	2.72	2.55	2.79
$Ser64O_\gamma-CclC_c$	1.31	1.32	1.39	1.45	1.49	1.75	2.60
$Tyr150O_\eta-Lys67N_\zeta$	2.80	2.77	2.90	2.96	3.18	3.20	3.55
$Tyr150O_\eta-Lys67H_{\zeta1}$	1.81	1.74	1.90	1.96	2.62	2.63	3.31
$Tyr150O_\eta-Lys315N_\zeta$	2.86	2.82	3.17	3.23	2.99	2.95	2.84
$Tyr150O_\eta-Lys315H_{\zeta2}$	2.42	1.80	2.18	2.24	1.99	1.96	1.85
$Lys315N_\zeta-Wat2O_w$	2.70	2.79	2.70	2.68	2.69	2.69	2.72
$Lys315H_{\zeta1}-Wat2O_w$	2.01	1.81	1.69	1.66	1.66	1.66	1.69
$Glu272O_{\epsilon1}-Wat2O_w$	2.97	2.67	2.63	2.62	2.61	2.62	2.61
$Glu272O_{\epsilon1}-Wat2H_{w1}$	2.30	1.72	1.68	1.67	1.66	1.67	1.66
$CclO_c-Ser64N$	2.93	3.02	3.01	2.93	2.85	2.86	3.09
$CclO_c-Ala318N$	3.00	2.94	2.91	2.82	3.06	3.03	2.80

$Lys315N_\zeta$, and $Wat2O_w$. A model compound for quantum chemical calculations was constructed by using this energy-minimized structure. Residues important for the substrate deacylation were considered in detail. Beadle et al. proposed that important residues for stabilization and function of the enzyme were Ser64, Lys67, Tyr150, Asn152, and Lys315,[42] while Powers et al. proposed that important residues for substrate recognition were Leu119, Asn152, Leu293, Ala318, Asn346, and Arg349.[43] From these residues, substrate-bound Ser64, Lys67, Tyr150, and Ala318, which exist in the catalytic center, and Glu272 and Lys315, which contribute to maintenance of the catalytic center, were selected to construct a model compound. Tyr150 will work as a general base. Ala318 as well as Ser64 contribute to the formation of an oxyanion hole. Lys67 interacts with Ser64 and Tyr150. Lys315 interacts with Tyr150. Glu272 interacts with Lys315 via a water molecule. The model compound was constructed by extracting the atoms shown by ball representation in Figure 1 and by substituting the atoms shown by asterisks with hydrogen atoms. The structures are shown in Figures 3−5 and S1 (in the Supporting Information). The number of atoms and degrees of freedom are 72 $[(C_{18}H_{41}N_4O_9)^-]$ and 210, respectively. Despite the long side chain of lysine, Lys67 and Lys315 were replaced with a short side chain, CH_3NH_3. It is thought that the influence of this replacement is negligible because the positively charged side chain of these residues strongly interacts with the negatively charged side chain of Glu272 (via a water molecule), Ser64, or Tyr150.

2.2. Computational Details. The Schrödinger equations for the model reaction system were solved by the ab initio MO method at the Hartree−Fock (HF) level. The basis set used was 6-31G**. The active site of a protein is surrounded by many molecules or residues. To consider this effect, the self-consistent reaction field theory based on the Onsager reaction field model[20−22] was adopted in this study. The radius of a cavity (a_0) was 5.98 Å, as determined from the volume of the model compound, and the dielectric constant was 20.0, which is appropriate to describe the ionic environment inside a protein.[44,45] Our previous works[19,46−50] showed that many enzymatic reactions were described properly by using this value.

Using the model compound mentioned in the previous subsection, the deacylation mechanism of class C β-lactamase was solved as follows. First, the transition state (TS) structure on the potential energy hypersurface was obtained by the energy gradient method. Normal frequency analysis was performed on the TS structure to confirm that a vibrational mode with only one imaginary frequency corresponded to the forward or reverse direction of the reaction. Next, intrinsic reaction coordinate (IRC) calculation[51] was performed from the TS structure to obtain the shortest path with the lowest energy level. In these calculations, the atoms shown by asterisks in Figure 3 (TS2) were fixed at their initial positions because of maintenance of enzymatic characteristics. The number of fixed atoms is 27. Potential energy calculations on several stationary point structures along the reaction path were performed by the DFT method. The exchange and correlation terms adopted were Becke's three-parameter functional[52] and Lee−Yang−Parr's formula,[53] respectively. The basis set used was the same as the one used in the HF calculation, 6-31G**. The computational program used was Gaussian 98.[41]

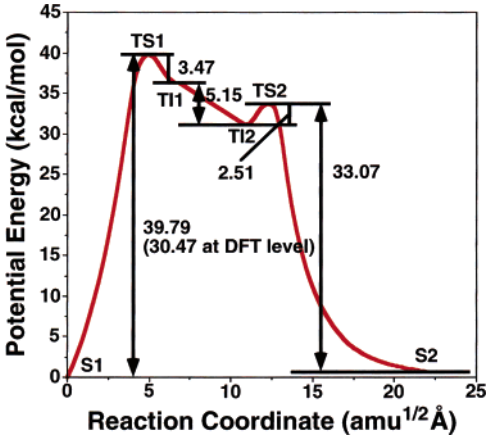

Figure 2. Profile of the lowest energy path along the IRC. Vertical and horizontal axes are potential energy (kcal/mol) and reaction coordinate (amu$^{1/2}$ Å), respectively.

3. Results

It was found that substrate deacylation of class C β-lactamase consisted of two elementary processes: (1) the formation of a tetrahedral intermediate structure and (2) the detachment of a hydroxylated substrate from the enzyme. The potential energy change is shown in Figure 2, and TS and minimum structures on the potential energy hypersurface are shown in Figures 3−5 and S1 (in the Supporting Information). Important interatomic distances in each reaction are shown in Table 1.

3.1. Tetrahedral Intermediate Formation. The first elementary process was the acyl−enzyme tetrahedral intermediate (TI) formation. The TS structure [Figure 3 (TS1)] was obtained by using the model compound extracted from the energy-minimized structure of a whole enzyme. Distances between $Wat1O_w$ and $CclC_c$ and between $Wat1O_w$ and $Tyr150O_\eta$ were 1.77 and 2.51 Å, respectively [Table 1 (TS1)]. It can be seen in the structure that an acyl−enzyme tetrahedral intermediate is formed. The arrows in this figure represent the directions of the vibrational mode with only one imaginary frequency calculated by normal vibrational analysis. The vibrational direction is toward the TI formation in which $Tyr150O_\eta$ abstracts H_{w1} of a water molecule, Wat1, that will be directly involved in deacylation. Starting from the TS structure, the initial structure of the deacylation reaction (S1) and the acyl−enzyme tetrahedral intermediate structure (TI1) were obtained by IRC calculations. S1 and TI1 are shown in Figure 4. In the S1 structure, $Wat1O_w$ interacts with a carbonyl carbon atom of the substrate ($CclC_c$) by 2.47 Å and with $Tyr150O_\eta$ by a hydrogen bond (2.69 Å).

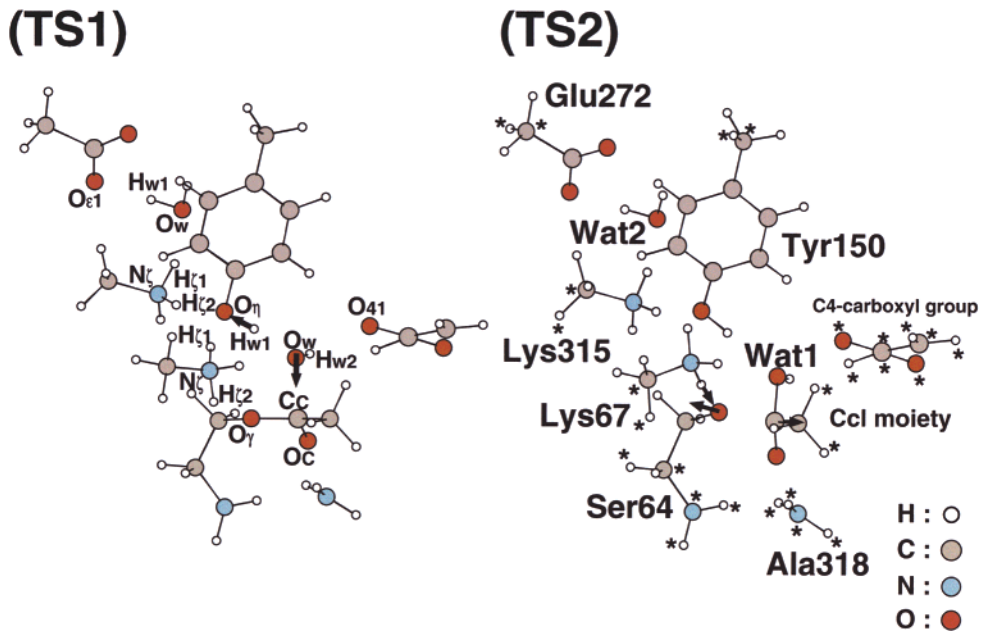

Figure 3. Two TS structures (TS1 and TS2). Arrows indicate vibrational modes obtained by normal frequency analysis. Atoms shown by asterisks were fixed during all quantum chemical calculations. Atom names and residue names are shown in TS1 and TS2, respectively.

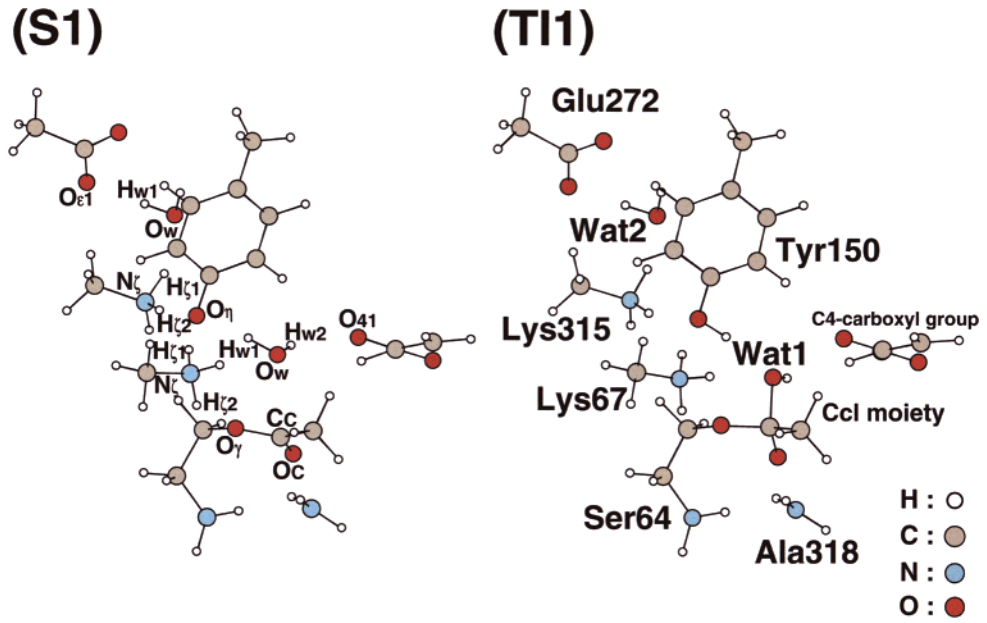

Figure 4. Initial structure (S1) and tetrahedral intermediate structure (TI1) obtained by IRC calculations. Atom names and residue names are shown in S1 and TI1, respectively.

Tyr150O_η is stabilized in the deprotonated state in the structure of the acyl-enzyme complex. This oxygen anion is stably held by Lys67N_ζ and Lys315N_ζ through hydrogen bonds whose distances are 2.77 and 2.82 Å, respectively (Table 1). The side chain of Tyr150 is usually neutral, but, in this case, it can exist in a negatively charged state due to the interaction with two positively charged side chains (two lysine residues). The oxygen anion has the ability to abstract a proton from a water molecule (the first elementary process). For this reason, it is thought that Tyr150 of class C enzyme works as a general base instead of an acidic residue like Glu166 of class A. The S1 structure almost reproduces the energy-minimized one by MM calculation except that the hydrogen bond between Wat1 and CclO_{41} atom is broken [3.24 Å, Table 1 (S1)]. In the TI structure, Wat1 is dissociated into a proton and a hydroxyl ion. The proton and the hydroxyl ion make covalent bonds with Tyr150O_η (0.97 Å) and CclC_c (1.48 Å), respectively [Table 1 (TI1)]. Wat1O_w interacts with Tyr150O_η by a hydrogen bond [2.77 Å, Table 1 (TI1)]. The activation energy of this process is 39.79 kcal/mol at the HF level (Figure 2). No significant change in interatomic distance was seen in the hydrogen-bond network of Tyr150O_η−Lys315N_ζ−Wat2O_w−Glu272$O_{\epsilon 1}$ and the oxyanion hole (CclO_c−Ser64N and CclO_c−Ala318N) (Table 1).

3.2. Detachment of Hydroxylated Substrate. The second elementary process was the detachment of a hydroxylated substrate assisted by the movement of Lys67$H_{\zeta 2}$ from Lys67 to Ser64. The TS structure [Figure 3 (TS2)] was obtained by the same method as that described the previous subsection. The distance between Lys67$H_{\zeta 2}$ and Ser64O_γ decreased from 2.05 Å of the TI1 structure to 1.45 Å, while the distance between Ser64O_γ and CclC_c increased from 1.45 Å for the TI1 structure to 1.75 Å [Table 1 (TS2)]. It can be seen in the structure that the hydroxylated substrate is detaching from the enzyme. The arrows in this figure represent the directions of the vibrational

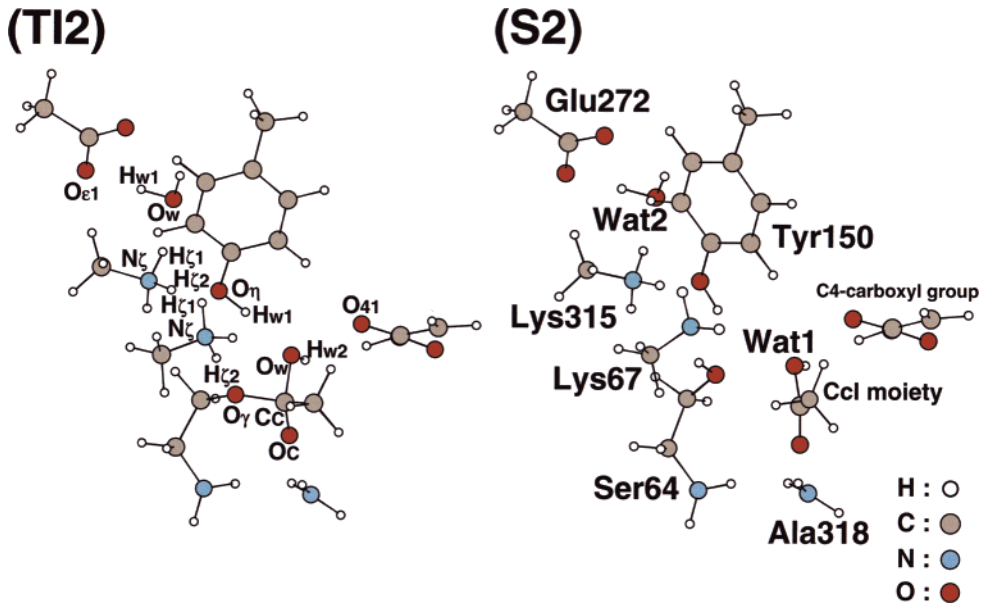

Figure 5. Reactant (TI2) and product (S2) in the detachment reaction of a hydroxylated substrate from the enzyme, which were obtained by IRC calculations. Atom names and residue names are shown in TI2 and S2, respectively.

SCHEME 3: Deacylation Mechanism by Class C β-lactamase Proposed in This Study

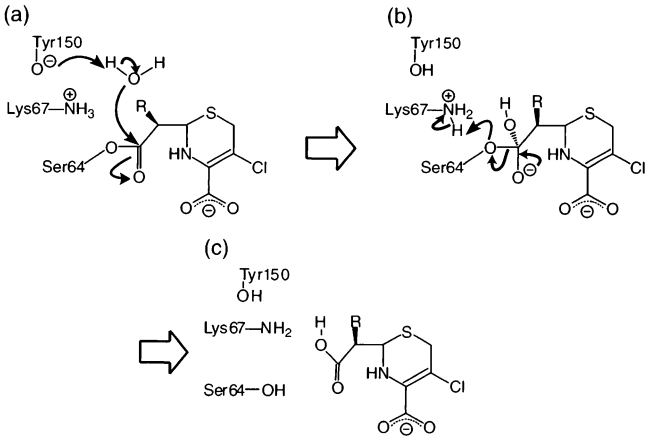

mode with only one imaginary frequency calculated by normal vibrational analysis. The vibrational direction is toward the formation of the final structure S2, in which Ser64O_γ abstracts Lys67$H_{\zeta 2}$ after substrate detachment from Ser64. Starting from the TS2 structure, the acyl−enzyme tetrahedral intermediate structure (TI2) and the product structure (S2) were obtained by IRC calculation. TI2 and S2 are shown in Figure 5. The TI2 structure differs from the TI1 structure and has an energetic advantage of about 5 kcal/mol compared with the TI1 structure. These two TI structures will be discussed in the next section. In the S2 structure, a covalent bond between ClC_c and Ser64O_γ is broken (2.60 Å). The activation energy of this process is 2.51 kcal/mol at the HF level (Figure 2). No prominent distance change is seen in the hydrogen-bond network of Tyr150O_η−Lys315N_ζ−Wat2O_w−Glu272$O_{\epsilon 1}$ and the oxyanion hole (ClO_c−Ser64N and CcO_c−Ala318N) (Table 1).

4. Discussion

The deacylation mechanism of class C β-lactamase was clarified in this study. The scheme is shown in Scheme 3(a to c). In the initial state a, the side chain of Tyr150 is charged negatively. The acyl−enzyme tetrahedral intermediate (b) is formed by the abstraction of a proton from a water molecule by the negative charge of the Tyr150 side chain followed by the connection of the resting hydroxyl ion to a carbonyl carbon atom of the substrate. Next, the substrate is detached from the enzyme by proton movement from Lys67 to Ser64O_γ (Scheme 2, c). The detached substrate is an inactive drug because of the opening of its β-lactam ring.

It is thought that there are four main mechanisms underlying antibiotic resistance of resistant bacteria: (1) inactivation of antibiotics by an enzyme that decomposes antibiotics, (2) change in the permeability of antibiotics to bacterial cells, (3) change in the metabolic process of bacteria, and (4) lowering of the affinity between antibiotics and the point of application. Class C β-lactamase contributes to antibiotic resistance by mechanism 1.

In the following sections, the reaction mechanism will be discussed in detail.

4.1. Tyr150 as a General Base. As seen in Figure 4 (S1), Tyr150O_η is stabilized in the deprotonated state in the structure of an acyl−enzyme complex. This oxygen anion is stably held by Lys67N_ζ and Lys315N_ζ through hydrogen bonds whose distances were 2.77 and 2.82 Å, respectively (Table 1). The side chain of Tyr150 is usually neutral, but in this case, it can exist in a negatively charged state due to interaction with two positively charged side chains (two lysine residues). The oxygen anion has the ability to abstract a proton from a water molecule (the first elementary process). For this reason, it is thought that Tyr150 of class C enzyme works as a general base instead of an acidic residue like Glu166 of class A. Dubus et al. suggested from the results of site-directed mutagenesis experiments[5,54] and measurements of enzymatic stability and activity[5] that Tyr150 plays an important role in the deacylation process. Lamotte-Brasseur et al. also suggested from measurement of pK_a of Tyr150 that Tyr150 works as a general base because Tyr150 showed a lower pK_a value than the values of other tyrosine residues.[29] The speculations based on these results are compatible with our theoretical results.

Recently, Gherman et al. proposed a Tyr150/Lys67 general base mechanism for the tetrahedral intermediate formation in the deacylation of class C β-lactamase: i.e., the side chains of Tyr150 and Lys67 are neutral in the initial state of deacylation and a proton relay from the water molecule for deacylation to

TABLE 2: Protonation Configurations and Relative Energies for the Acyl−Enzyme Intermediate

				relative energy (kcal/mol)		
config	Tyr150	Lys67	Lys315	B3LYP/ 6-31G**	B3LYP/ 6-311++G**	MP2/ 6-31G**
1	protonated	protonated	deprotonated	6.39	7.11	7.68
2[a]	protonated	deprotonated	protonated	0.76	3.00	1.53
3[b]	deprotonated	protonated	protonated	0.00	0.00	0.00

[a] Tyr150/Lys67 general base mechanism. [b] Tyr150 general base mechanism.

Lys67 via Tyr150 occurs in the tetrahedral intermediate formation.[30] We also calculated the initial structure of the Tyr150/Lys67 general base mechanism. The potential energy of the structure was 0.76 kcal/mol higher than that of the Tyr150 general base mechanism (this study) at the DFT level. Calculation using another basis set and higher order calculation also showed that the structure had a higher level of potential energy than that of the Tyr150 general base mechanism (Table 2, configuration 2). The protonated Tyr150/deprotonated Lys315 structure had a much higher level of potential energy than that of the initial structure of the Tyr150/Lys67 general base mechanism (Table 2, configuration 1). It is thought that configuration 1 in Table 2 is not involved in the deacylation mechanism of class C β-lactamase. These results agree qualitatively with Ghermans' results, and MP2/6-31G** results are almost the same as their results.[30] It is necessary to determine whether the structure in which both Tyr150 and Lys67 are neutral is produced as a result of the acylation process. For this reason, only the Tyr150 general base mechanism was considered in this study. The acylation process will be discussed elsewhere.

Since Tyr150 plays an important role in the deacylation process, chemicals that inhibit the action of this residue might become candidates for new medicine. Many antibiotics have been developed by changing the functional groups that combine with the basic skeleton. If the development is advanced from the viewpoint of direct inhibition of catalytic residues around a serine residue in the active center, new potent medicine might be discovered.

4.2. Two Tetrahedral Intermediate Structures. The TI1 structure obtained by IRC calculation starting from the TS1 structure differs from the TI2 structure obtained by IRC calculation starting from the TS2 structure. As shown in Table 1, the distances between $Lys67N_{\zeta}$ and $Tyr150O_{\eta}$, between $Lys315N_{\zeta}$ and $Tyr150O_{\eta}$, and between $Lys67H_{\zeta 2}$ and $Ser64O_{\gamma}$ in TI1 are 2.96, 3.23, and 2.05 Å, respectively, whereas those distances in TI2 are 3.18, 2.99, and 1.68 Å, respectively. No prominent change is seen in other distances between the two structures. The major difference between TI1 and TI2 structures is that, in the TI2 structure, Lys67 is slightly away from Tyr150 and, consequently, $Lys67H_{\zeta 2}$ approaches $Ser64O_{\gamma}$, while Lys315 approaches Tyr150 (Figures 4 and 5). Moreover, a hydrogen bond between $Lys67N_{\zeta}$ and $Ser64O_{\gamma}$ is formed in the TI2 structure but not in the TI1 structure. These structural differences suggest that the second elementary process occurs more easily from TI2 than from TI1. No noticeable potential barrier was observed between the two structures. The potential energy of TI2 is about 5 kcal/mol lower than that of TI1. For this reason, the structural change from TI1 to TI2 will occur spontaneously, and TI2 is thought to be the real tetrahedral intermediate structure. The existence of the TI1 structure in this study may originate in the achievement at the criteria of the stationary point before going to TI2 due to some fixation in the model.

4.3. Roles of Lys67 and Lys315. As shown in Table 1, $Lys315N_{\zeta}$ moves away from $Tyr150O_{\eta}$ (S1, 2.82 Å → TS1, 3.17 Å → TI1, 3.23 Å) in the first elementary process, but it returns back to make a hydrogen bond (TI2, 2.99 Å → TS2, 2.95 Å → S2, 2.84 Å) in the second elementary process. $Lys67N_{\zeta}$ gradually moves away from $Tyr150O_{\eta}$ with progress of the reaction (S1, 2.77 Å → TS1, 2.90 Å → TI1, 2.96 Å → TI2, 3.18 Å → TS2, 3.20 Å → S2, 3.55 Å). That is to say, both $Lys67N_{\zeta}$ and $Lys315N_{\zeta}$ move away from $Tyr150O_{\eta}$, in accordance with the abstraction of a proton from Wat1 by $Tyr150O_{\eta}$ in the first elementary process, but $Lys315N_{\zeta}$ approaches $Tyr150O_{\eta}$ again when $Lys67N_{\zeta}$ approaches $Ser64O_{\gamma}$ and goes further away from $Tyr150O_{\eta}$ in the second elementary process. For this reason, it is thought that amino groups of the side chains of Lys67 and Lys315 cooperatively fix the location of the side chain of Tyr150. Monnaie et al. suggested from the results of a site-directed mutagenesis experiment that Lys67 plays an important role in the enzymatic activity, particularly in control of the electrostatic environment.[55] They also performed another site-directed mutagenesis experiment on Lys315 and reported that this residue mainly enhanced nucleophilic attack.[56] Their conclusion based on these results is also consistent with our theoretical results.

4.4. Proton Transfer from Tyr150 to Lys67. The side chain of Tyr150 is in a protonated state in the S2 structure, whereas that of Lys67 is in a deprotonated state. Does the proton of Tyr150 transfer to Lys67? We tried to determine the TS structure (TS3) of the proton-transfer reaction and obtained reactant (S2) and product (S3) structures by IRC calculations after normal frequency analysis of the TS3 structure. The structures and interatomic distances of TS3 and S3 are shown in Figure S1 and Table S1 in the Supporting Information, respectively. The distance between $Wat1H_{w1}$ and $Lys67N_{\zeta}$ decreased from 3.18 Å for the S2 structure to 1.15 Å, while the distance between $Wat1H_{w1}$ and $Tyr150O_{\eta}$ increased from 0.96 Å for the S2 structure to 1.36 Å [Table S1 (TS3)]. It can be seen in the structure that the proton is transferring from Tyr150 to Lys67 [Figure S1 (TS3)]. The proton transfer is completed in the S3 structure. The reaction, however, needs a large amount of activation energy (25.96 kcal/mol), and moreover, the potential energy of the S3 structure is 24.48 kcal/mol higher than that of the S2 structure. This suggests that the proton transfer from Tyr150 to Lys67 does not occur at the last stage of the deacylation reaction. Instead, deprotonation of the Tyr150 side chain and protonation of the Lys67 side chain might occur in the resting state after the release of the hydroxylated substrate from the enzyme or in the acylation reaction for the next substrate in the enzymatic reaction cycle of class C β-lactamase. Kato-Toma et al. suggested from pK_a measurements from NMR that Tyr150 in class C β-lactamase of *Citrobacter freundii* GN346 is protonated in a substrate-free form.[57] Their speculation is compatible with our speculation.

4.5. Potential Energy Change for Deacylation of Class C β-Lactamase. As shown in Figure 2, the activation energies of the first and second elementary processes are 39.79 and 2.51 kcal/mol, respectively; i.e., the former is the rate-determining process. Once the tetrahedral intermediate is produced, detachment of the hydroxylated substrate will occur easily, because

the potential energy of TS2 is lower than that of TS1. The activation energy of the rate-determining process was estimated to be 30.47 kcal/mol from DFT calculations considering electron correlation. Calculations by other methods (MP2/6-31G** and B3LYP/6-311++G**) also gave the same results (31.76 and 31.12 kcal/mol), and it is thought that these values are reliable. Gherman et al. estimated the activation energy to be 21.5 kcal/mol by QM/MM calculation.[30] Fujii et al. reported that the activation energy of the rate-determining step of the deacylation of class A β-lactamase was 24.55 kcal/mol.[19] Other activation energies of the rate-determining process of enzymatic reactions that proceeded via a tetrahedral intermediate were 41.97 kcal/mol for the hydrolysis of ATP by myosin[58] and 23.95 kcal/mol for the site-specific hydrolysis of a Phe-Pro peptide bond by HIV-1 protease.[59] The value obtained in this study is the same level as these results.

5. Conclusions

The deacylation mechanism of class C β-lactamase was clarified by using quantum chemical calculations. It was found that the mechanism consisted of two elementary processes. The first process was tetrahedral intermediate formation, which was initiated by the activation of catalytic water by Tyr150, and the second process was detachment of a hydroxylated substrate from the enzyme, which was associated with proton transfer from the side chain of Lys67 to Ser64O_γ. From the viewpoint of substrate deacylation, a key factor of class C β-lactamase is that the deprotonated side chain of Tyr150 is stably present in the catalytic center of the acyl−enzyme complex and is held by Lys67 and Lys315 cooperatively.

Acknowledgment. This work was partly supported by a Grant-in-Aid for Young Scientists (B) [KAKENHI(14771305)] and for Center of Excellence (COE) research from The Ministry of Education, Culture, Sports, Science and Technology (MEXT). The authors thank the Computer Center of the Institute for Molecular Science, for the use of Fujitsu VPP5000 computer. The computations were also carried out by the DRIA system at Graduate School of Pharmaceutical Sciences, Chiba University.

Supporting Information Available: Structures (Figure S1) and table of interatomic distances (Table S1) of TS3 and S3. This material is available free of charge via the Internet at http://pubs.acs.org.

References and Notes

(1) Livermore, D. M. *Clin. Microbiol. Rev.* **1995**, *8*, 557−584.
(2) Bush, K.; Jacoby, G.; Medeiros, A. *Antimicrob. Agents Chemother.* **1995**, *39*, 1211−1233.
(3) Gibson, R. M.; Christensen, H.; Waley, S. G. *Biochem. J.* **1990**, *272*, 613−619.
(4) Strynadka, N. C. J.; Adachi, H.; Jensen, S. E.; Johns, K.; Sielecki, A.; Betzel, C.; Sutoh, K.; James, M. N. G. *Nature* **1992**, *359*, 700−705.
(5) Dubus, A.; Ledent, P.; Lamotte-Brasseur, J.; Frère, J.-M. *Proteins: Struct., Funct., Genet.* **1996**, *25*, 473−485.
(6) Guillaume, G.; Vanhove, M.; Lamotte-Brasseur, J.; Ledent, P.; Jamin, M.; Joris, B.; Frere, J.-M. *J. Biol. Chem.* **1997**, *272*, 5438−5444.
(7) Nukaga, M.; Mayama, K.; Hujer, A. M.; Bonomo, R. A.; Knox, J. R. *J. Mol. Biol.* **2003**, *328*, 289−301.
(8) Wilkinson, A.-S.; Bryant, P. K.; Meroueh, S. O.; Page, M. G. P.; Mobashery, S.; Wharton, C. W. *Biochemistry* **2003**, *42*, 1950−1957.
(9) Pagan-Rodriguez, D.; Zhou, X.; Simmons, R.; Bethel, C. R.; Hujer, A. M.; Helfand, M. S.; Jin, Z.; Guo, B.; Anderson, V. E.; Ng, L. M.; Bonomo, R. A. *J. Biol. Chem.* **2004**, *279*, 19494−19501.
(10) Ishiguro, M.; Imajo, S. *J. Med. Chem.* **1996**, *39*, 2207−2218.
(11) Díaz, N.; Suárez, D.; Sordo, T. L.; Merz, K. M., Jr. *J. Phys. Chem. B* **2001**, *105*, 11302−11313.
(12) Massova, I.; Kollman, P. A. *J. Comput. Chem.* **2002**, *23*, 1559−1576.
(13) Díaz, N.; Sordo, T. L.; Merz, K. M., Jr.; Suárez, D. *J. Am. Chem. Soc.* **2003**, *125*, 672−684.
(14) Hermann, J. C.; Ridder, L.; Mulholland, A. J.; Höltje, H.-D. *J. Am. Chem. Soc.* **2003**, *125*, 9590−9591.
(15) Fenollar-Ferrer, C.; Frau, J.; Donoso, J.; Muñoz, F. *Proteins* **2003**, *51*, 442−452.
(16) Oliva, M.; Dideberg, O.; Field, M. J. *Proteins* **2003**, *53*, 88−100.
(17) Hermann, J. C.; Hensen, C.; Ridder, L.; Mulholland, A. J.; Höltje, H.-D. *J. Am. Chem. Soc.* **2005**, *127*, 4454−4465.
(18) Hata, M.; Fujii, Y.; Ishii, M.; Hoshino, T.; Tsuda, M. *Chem. Pharm. Bull.* **2000**, *48*, 447−453.
(19) Fujii, Y.; Hata, M.; Hoshino, T.; Tsuda, M. *J. Phys. Chem. B* **2002**, *106*, 9687−9695.
(20) Onsager, L. *J. Am. Chem. Soc.* **1936**, *58*, 1486-1493.
(21) Tapia, O.; Goscinski, O. *Mol. Phys.* **1975**, *29*, 1653−1661.
(22) Wong, M. W.; Frisch, M. J.; Wiberg, K. B. *J. Am. Chem. Soc.* **1991**, *113*, 4776−4782.
(23) Oefner, C.; D'Arcy, A.; Daly, J. J.; Gubernator, K.; Charnas, R. L.; Heinze, I.; Hubschwerlen, C.; Winkler, F. K. *Nature* **1990**, *343*, 284−288.
(24) Patera, A.; Blaszczak, L. C.; Shoichet, B. K. *J. Am. Chem. Soc.* **2000**, *122*, 10504−10512.
(25) Lobkovsky, E.; Moews, P.; Liu, H.; Zhao, H.; Frere, J.; Knox, J. *Proc. Natl. Acad. Sci. U.S.A.* **1993**, *90*, 11257−11261.
(26) Wouters, J.; Fonzé, E.; Vermeire, M.; Frère, J.-M.; Charlier, P. *Cell. Mol. Life Sci.* **2003**, *60*, 1764−1773.
(27) Nukaga, M.; Abe, T.; Venkatesan, A. M.; Mansour, T. S.; Bonomo, R. A.; Knox, J. R. *Biochemistry* **2003**, *42*, 13152−13159.
(28) Nukaga, M.; Kumar, S.; Nukaga, K.; Pratt, R. F.; Knox, J. R. *J. Biol. Chem.* **2004**, *279*, 9344−9352.
(29) Lamotte-Brasseur, J.; Dubus, A.; Wade, R. C. *Proteins* **2000**, *40*, 23−28.
(30) Gherman, B. F.; Goldberg, S. D.; Cornish, V. W.; Friesner, R. A. *J. Am. Chem. Soc.* **2004**, *126*, 7652−7664.
(31) Guallar, V.; Baik, M.-H.; Lippard, S. J.; Friesner, R. A. *Proc. Natl. Acad. Sci. U.S.A.* **2003**, *100*, 6998−7002.
(32) Schöneboom, J. C.; Cohen, S.; Lin, H.; Shaik, S.; Thiel, W. *J. Am. Chem. Soc.* **2004**, *126*, 4017−4034.
(33) Guallar, V.; Friesner, R. A. *J. Am. Chem. Soc.* **2004**, *126*, 8501−8508.
(34) Lin, H.; Schöneboom, J. C.; Cohen, S.; Shaik, S.; Thiel, W. *J. Phys. Chem. B* **2004**, *108*, 10083−10088.
(35) Berman, H. M.; Westbrook, J.; Feng, Z.; Gilliland, G.; Bhat, T. N.; Weissig, H.; Shindyalov, I. N.; Bourne, P. E. *Nucleic Acids Res.* **2000**, *28*, 235−242.
(36) Meyers, B. R. *Clin. Ther.* **2000**, *22*, 154−166.
(37) Jorgensen, W. L.; Chandrasekhar, J.; Madura, J. D.; Impey, R. W.; Klein, M. L. *J. Chem. Phys.* **1983**, *79*, 926−935.
(38) Case, D. A.; Pearlman, D. A.; Caldwell, J. W.; Cheatham, T. E., III; Ross, W. S.; Simmerling, C. L.; Darden, T. A.; Merz, K. M.; Stanton, R. V.; Cheng, A. L.; Vincent, J. J.; Crowley, M.; Tsui, V.; Radmer, R. J.; Duan, Y.; Pitera, J.; Massova, I.; Seibel, G. L.; Singh, U. C.; Weiner, P. K.; Kollman, P. A. *AMBER 6*; University of California: San Francisco, 1999.
(39) Bayly, C. I.; Cieplak, P.; Cornell, W.; Kollman, P. A. *J. Phys. Chem.* **1993**, *97*, 10269−10280.
(40) Singh, U. C.; Kollman, P. A. *J. Comput. Chem.* **1984**, *5*, 129−145.
(41) Frisch, M. J.; Trucks, G. W.; Schlegel, H. B.; Scuseria, G. E.; Robb, M. A.; Cheeseman, J. R.; Zakrzewski, V. G.; Montgomery, J. A., Jr.; Stratmann, R. E.; Burant, J. C.; Dapprich, S.; Millam, J. M.; Daniels, A. D.; Kudin, K. N.; Strain, M. C.; Farkas, O.; Tomasi, J.; Barone, V.; Cossi, M.; Cammi, R.; Mennucci, B.; Pomelli, C.; Adamo, C.; Clifford, S.; Ochterski, J.; Petersson, G. A.; Ayala, P. Y.; Cui, Q.; Morokuma, K.; Salvador, P.; Dannenberg, J. J.; Malick, D. K.; Rabuck, A. D.; Raghavachari, K.; Foresman, J. B.; Cioslowski, J.; Ortiz, J. V.; Baboul, A. G.; Stefanov, B. B.; Liu, G.; Liashenko, A.; Piskorz, P.; Komaromi, I.; Gomperts, R.; Martin, R. L.; Fox, D. J.; Keith, T.; Al-Laham, M. A.; Peng, C. Y.; Nanayakkara, A.; Challacombe, M.; Gill, P. M. W.; Johnson, B.; Chen, W.; Wong, M. W.; Andres, J. L.; Gonzalez, C.; Head-Gordon, M.; Replogle, E. S.; Pople, J. A. *Gaussian 98, Revision A.11*; Gaussian, Inc.: Pittsburgh, PA, 2001.
(42) Beadle, B. M.; Shochet, B. K. *J. Mol. Biol.* **2002**, *321*, 285−296.
(43) Powers, R. A.; Shochet, B. K. *J. Med. Chem.* **2002**, *45*, 3222−3234.
(44) Antosiewicz, J.; McCammon, J. A.; Gilson, M. K. *Biochemistry* **1996**, *35*, 7819−7833.
(45) Sham, Y. Y.; Muegge, I.; Warshel, A. *Biophys. J.* **1998**, *74*, 1744−1753.
(46) Hata, M.; Hirano, Y.; Hoshino, T.; Tsuda, M. *J. Am. Chem. Soc.* **2001**, *123*, 6410−6416.

(47) Hirano, Y.; Hata, M.; Hoshino, T.; Tsuda, M. *JCPE J.* **2000**, *12*, 119−128.
(48) Hirano, Y.; Hata, M.; Hoshino, T.; Tsuda, M. *J. Phys. Chem. B* **2002**, *106*, 5788−5792.
(49) Murata, K.; Fujii, Y.; Enomoto, N.; Hata, M.; Hoshino, T.; Tsuda, M. *Biophys. J.* **2000**, *79*, 982−991.
(50) Murata, K.; Hoshino, T.; Sato, Y.; Hata, M.; Tsuda, M. *Chem-Bio Inform. J.* **2002**, *2*, 97−103.
(51) Fukui, K. *Acc. Chem. Res.* **1981**, *14*, 363−368.
(52) Becke, A. D. *J. Chem. Phys.* **1993**, *98*, 5648−5652.
(53) Lee, C.; Yang, W.; Parr, R. G. *Phys. Rev. B* **1988**, *37*, 785−789.
(54) Dubus, A.; Normark, S.; Kania, M.; Page, M. G. P. *Biochemistry* **1994**, *33*, 8577−8586.
(55) Monnaie, D.; Dubus, A.; Frere, J. M. *Biochem. J* **1994**, *302*, 1−4.
(56) Monnaie, D.; Dubus, A.; Cooke, D.; Marchand-Brynaert, J.; Normark, S.; Frere, J.-M. *Biochemistry* **1994**, *33*, 5193−5201.
(57) Kato-Toma, Y.; Iwashita, T.; Masuda, K.; Oyama, Y.; Ishiguro, M. *Biochem. J.* **2003**, *371*, 175−181.
(58) Okimoto, N.; Yamanaka, K.; Ueno, J.; Hata, M.; Hoshino, T.; Tsuda, M. *Biophys. J.* **2001**, *81*, 2786−2794.
(59) Okimoto, N.; Tsukui, T.; Hata, M.; Hoshino, T.; Tsuda, M. *J. Am. Chem. Soc.* **1999**, *121*, 7349−7354.